Fungi present distinguishable isotopic signals in their lipids when grown on glycolytic versus tricarboxylic acid cycle intermediates

Stanislav Jabinski[1,2] Vítězslav Kučera[3,4], Marek Kopáček[1,5], Jan Jansa[4], Travis B. Meador[1,2,5*]

[1]University of South Bohemia, Faculty of Science, Department of Ecosystem Biology, Branišovská 1760, 370 05 České Budějovice, Czechia

[2]Institute of Soil Biology and Biochemistry, Biology Centre CAS, Na Sádkách 7, 370 05 České Budějovice, Czechia

[3]Charles University, Faculty of Sciences, Albertov 6, 128 00 Praha, Czechia

[4]Institute of Microbiology CAS, Vídeňská 1083, 142 20 Praha, Czechia

[5]Institute of Hydrobiology, Biology Centre CAS, Na Sádkách 7, 370 05 České Budějovice, Czechia

Correspondence to: Travis B. Meador (travis.meador@bc.cas.cz)

Abstract. Microbial activity in soils controls both the size and turnover rates of large carbon (C) inventories stored in the subsurface, having important consequences for partitioning of C between terrestrial and atmospheric reservoirs as well as recycling of mineral nutrients such as nitrogen or phosphorus (often bound to the C) that support plant growth. Fungi are major decomposers of soil organic matter (SOM); however, uncertainty about the identity of predominant C substrates that fuel their respiration confound models of fungal production and SOM turnover. To further define the signals of microbial heterotrophic activity, we applied a dual hydrogen (H) and C stable isotope probing (SIP) approach on pure fungal cultures representing the phyla Ascomycota, Basidiomycota, and Zygomycota growing on monomeric (glucose, succinate) or complex substrates (tannic acid, β-cyclodextrin). Our findings demonstrate that the investigated species incorporated only minor amounts of inorganic C (provided as bicarbonate) into their membrane lipids, amounting to < 3% of lipid-C, with no consistent patterns observed between species or growth substrates. The net incorporation of water-derived H (i.e., a_w) into lipids also did not differ significantly between incubations with monomeric versus complex substrates; however, growth on succinate elicited significantly higher a_w values than glucose or β-cyclodextrin. This finding suggests that ^{2}H-SIP assays have the potential to distinguish between microbial communities supported predominantly by substrates that are catabolized by the tricarboxylic acid cycle versus glycolytic pathway. Furthermore, the average a_w value of heterotrophic fungal incubations [0.69 ± 0.03 (SEM)] is consistent with that observed for bacterial heterotrophs, and may be applied for upscaling lipid-based estimates of fungal production in environmental assays.

Short Summary

Microbial production is a key parameter in estimations of organic matter cycling in environmental systems, and fungi play a major role as decomposers. In order to investigate fungal production and turnover times in soils, we incubated fungal pure cultures with isotopically labelled water and bicarbonate to investigate growth signals encoded into lipid biomarkers, which can be applied to improve flux estimates in environmental studies.

1 Introduction

Soil organic matter (SOM) is the major reservoir of carbon (1580×10^{15} g C) in the biosphere, and active microbial populations act to redistribute this C to other reactive reservoirs, such as the atmosphere (Carson et al., 2001; Grinhut et al., 2007). Major uncertainties in modeling C and climate dynamics stem from insufficient knowledge on the controls of SOM degradation and transformation (Ciais et al., 2014; Lindahl and Tunlid 2015). Saprotrophic soil fungi are one of the major decomposers in soils, are known to degrade naturally occurring complex molecules such as lignin (Kirk & Farrell, 1987; Fioretto et al., 2005; Baldrian et al., 2011), cellulose (Šnajdr et al., 2011) and humic substances (Grinhut et al., 2007), but are also reported to compete for accessible plant photosynthate excreted by roots (De Boer et al., 2005; Högberg et al., 2001; Smith & Read, 2008). Despite the unique and important fungal niche in biogeochemical cycles, their contributions to SOM cycling remains poorly constrained (Frey 2019; Grinhut et al., 2007). Furthermore, heterotrophic organisms feeding on organic substrates to gain energy and build biomass are also known to fix a variable amount of inorganic C (IC), in order to replenish intermediates in the tricarboxylic acid (TCA) cycle (Kornberg 1965). It has been suggested that 2 - 8% of the biomass C in heterotrophs originates from IC incorporated through anaplerotic carboxylation reactions (Romanenko 1964; Roslev et al., 2004; Braun et al., 2021). Awareness of these processes has existed for decades (Kornberg 1965; Sorotkin 1966). Yet, the relevance and metabolic controls on heterotrophic IC fixation remains poorly understood, partly due to the lack of reliable estimates for most organisms and habitats (Braun et al., 2021).

Advanced analytical techniques now allow microbial taxa to be linked to specific processes in environmental studies by measuring incorporation of stable isotopes into biomarkers (Boschker et al., 1998; Dumont and Murrell, 2005; Kreuzer-Martin, 2007), such as fungal and bacterial membrane lipid fatty acids (Treonis et al., 2004; Willers et al., 2015) or other biomarkers (Boschker and Middelbourg, 2002). Previous studies have demonstrated that variability in the $^{2/1}$H composition of microbial lipids is redundant with that of environmental water (Hoefs, 2018; Kopf et al., 2015), and stable isotope probing (SIP) assays applying enrichments in ^{2}H$_2$O have proven to be a useful tracer of microbial activity in a diverse range of environments (Canarini et al., 2024; Caro et al., 2023; Fischer et al., 2013; Kellermann et al., 2012; Wegener et al., 2016; Warren 2022; Wu et al., 2018). It is important to distinguish these ^{2}H-labeling applications from parallel investigations aiming to determine the kinetic and equilibrium isotope fractionations resulting from biosynthetic incorporation of water hydrogen (water-H) into individual compounds (i.e., ε; cf. Hayes 2004). While ε values can be indicative of an underlying metabolic processes or environmental change (Osborn et al., 2011; Sachse et al., 2012; Zhang et al., 2009), the large range of ε that have been reported

64 for fatty acids of aerobic, heterotrophic bacteria [$-330 > \varepsilon > +360$ ‰; see review by Pilecky et al. (2025)] arise, in part, because

65 water-H is not the only source of H for biomolecules, complicating the interpretation of such values observed in natural

66 systems. In contrast, the water-H incorporation factor (or water-H assimilation efficiency; a_w) accounts for variability in the

67 proportion of H derived from water as well as $^{2/1}H$ fractionation during biosynthesis (cf. Zhang et al., 2009; Kopf at al. 2015;

68 see Methods), and has been valuable for SIP approaches to (*i*) estimate microbial production rates in natural systems (e.g.,

69 Wegener et al., 2022; Caro et al., 2023), and (*ii*) establish characteristic growth patterns of microbial populations that can

70 access a large diversity of substrates, such as methanogens (Wu et al., 2020).

71 To fully exploit the potential of SIP experiments, a dual-SIP approach was developed to track total microbial production by

72 adding heavy water (^2H_2O) together with ^{13}C-labeled IC, enabling simultaneous estimates of total and autotrophic metabolism,

73 respectively (Wegener et al., 2012; Wu et al., 2020). Recently, Jabinski et al. (2024) validated an innovation of the dual-SIP

74 assay by using rapid pyrolysis of fungal biomass to determine the stable C and H isotopic composition of fungal lipids, and

75 demonstrated that water-H and IC assimilation signatures could successfully distinguish between fungal ecotypes growing on

76 glucose or glutamic acid as the C source. The aim of the current study was to further assess the controls on water-H and IC

77 incorporation into lipids and expand our knowledge for interpreting environmental signals by applying the dual-SIP assay on

78 a broader range of pure fungal cultures and growth substrates, including labile monomers versus more complex, high molecular

79 weight molecules. We hypothesized that (*i*) the incorporation of IC and water-H into the fungal fatty acid biomarker $C_{18:2}$ will

80 be similar for fungal species growing on the same substrate, and (*ii*) that IC and water-H incorporation will distinguish between

81 growth on labile versus more complex C substrates.

82 **2 Methods**

83 **2.1 Cultivation & Harvesting**

84 Fungal pure cultures of two Basidiomycota [*Paxillus involutus* (PI, strain SB-22); *Phanerodontia chrysosporium* (PC, strain

85 CCM8074)], two Zygomycota [*Mortierella* sp. (MO, strain RK-38); *Umbelopsis* sp. (UM, strain RK-43)] and two Ascomycota

86 [*Penicillium janczewskii* (PJ, strain BCCO20_0265); *Paecilomyces lilacinus* (PL, strain DP-23)] were incubated in 500 mL

87 Schott bottles at 25 °C in the dark. Liquid mineral media (50 mL) was adapted after Bukovská et al. (2018) with the vitamins

88 left out, and was inoculated with approximately 10^6 spores, or, for Basidiomycota, a hyphal block < 0.5 cm^3 recovered from a

89 previous culture using the same cultivation medium solidified with agar (1.5%).

90 The growth medium contained per liter: 4 g organic C in various forms ($C_6H_{12}O_6$ glucose; $C_4H_6O_4$ succinic acid; $C_{42}H_{70}O_{35}$ β-

91 Cyclodextrin or $C_{76}H_{52}O_{46}$ tannic acid), 0.01 g $FeSO_4 * 7H_2O$, 2 g KH_2PO_4, 0.5 g $MgSO_4 * 7H_2O$, 0.1 g NaCl, 0.1 g CaCl, 2.5

92 g $(NH_4)_2SO_4$, 0.45 g $NaHCO_3$ and 1 mL of a mixed solution (per liter: 0.5 g H_3BO_3, 0.04 g $CuSO_4 * 5H_2O$, 0.1 g KI, 0.4 g

93 $MnSO_4 * 5H_2O$, 0.2 g $NaMoO_4 * 2H_2O$, 0.4 g $ZnSO_4 * 7H_2O$). The pH of the medium was adjusted to 4.5 before inoculation.

94 Dual-SIP experiments were performed using ^{13}C-bicarbonate (^{13}C-DIC, $NaH^{13}CO_3$) and deuterated water (^2H_2O). Each fungal

95 strain was grown in triplicate with non-labeled substrates (Treatment I), with δ^2H of the medium water adjusted to 100‰ and

96 AT^{13}C = 10% of ^{13}C-DIC (Treatment II), 200‰ δ^2H and 10% ^{13}C-DIC (Treatment III), and 400‰ δ^2H and 10% ^{13}C-DIC

97 (Treatment IV). The concentration of the bicarbonate in the cultivation medium was 0.1 g L^{-1}. The Schott bottles were closed

98 with a rubber stopper in order to prevent the labeled ^{13}C-DIC from outgassing, and ample headspace was provided to maintain

99 oxic conditions throughout the growth experiment. Fungal growth was monitored via the accumulation of CO_2 in the

100 headspace, and we aimed to harvest when CO_2 levels reached 10%; however, without preliminary knowledge of the fungal

101 growth dynamics, some cultivations exceeded this level more quickly than they could be harvested.

102 To harvest the fungal biomass, mycelia were separated from the growth medium via vacuum filtration through 5 μm Isopore

103 polycarbonate filters (47 mm diam, Merck catalogue number TMTP04700) and the cultivation medium was collected into a

104 sterile 50 mL tube. Thereafter, the mycelium was washed with ample MilliQ water, transferred to pre-weighed, sterile 50 mL

105 tubes; the fresh weight of the biomass was recorded, and the samples were frozen at -80 °C until lyophilization. A subsample

106 of the cultivation medium was also frozen at -80 °C and the rest was used to determine pH post-incubation. After lyophilization,

107 the dry weight of each sample was determined and stored at -20 °C until further analysis.

2.2 Measurements

2.2.1 Headspace CO_2 concentration and isotope composition

111 Samples of headspace (0.3 mL) were collected weekly from each bottle into helium flushed 12 mL exetainer vials (Exetainer,

112 Labco Limited, UK) and analyzed for their CO_2 concentration and ^{13}C/^{12}C isotopic ratio using GasBench II equipped with a

113 single cryo-trap connected to Delta V Advantage isotopic ratio mass spectrometer (IRMS) via Conflo IV (Thermo Scientific,

114 Bremen, Germany). Ambient air (with its CO_2 concentration measured using LiCor 850 gas analyzer previously) was used as

115 a standard for CO_2 concentration measurements, whereas a laboratory cylinder with 0.1% CO_2 in helium was used as a standard

116 for isotopic composition (δ^{13}C = -2.86 ‰). The analytical precision was below 1‰. Data were analyzed and exported using

117 Isodat 3.0 software.

2.2.2 Medium water (^{2}H$_2$O)

119 Liquid samples were transferred into 1.5 ml glass vials (32 x 11.6 mm, Fischer Scientific) and then measured using Triple

120 Liquid Water Isotope Analyzer (Los Gatos Research), which is based on the principle of high-resolution laser absorption

121 spectroscopy. Samples were dispensed into the instrument using an autosampler (PAL3 LSI, ABB company) and a 1.2 μL

122 syringe (Hamilton). Samples were measured and evaluated against prepared laboratory standards of known isotopic

123 composition. The isotopic ratios of these laboratory standards were verified by measuring against international standards

124 (VSMOW2, SLAP2) made by the IAEA. For quality control purposes, the measurements of the samples were also interspersed

125 with periodic measurements of the prepared verification samples with known isotopic composition. The final isotopic

126 composition (δ^2H) was determined using LIMS software. Analytical precision of δ^2H was <1.5‰.

127 Water sampled from incubations with tannic acid could not be measured using the laser, as described above, due to its high

128 organic carbon content, and was rather measured via a GasBench II device (Thermo Scientific, Bremen, Germany; Application

129 Note: 30049). Medium water samples (200 µL) were added with a platinum catalyst to 12 mL exetainer vials (Exetainer, Labco

130 Limited, UK). The headspace was flushed with 1% H_2 in He at approximately 100 mL min^{-1} for 6 min. After an equilibration

131 time of over 40 min, the samples were measured by purging the exetainer using a double-holed needle with helium into a 250

132 µL sample loop. The sample was then injected and separated via a Carboxen PLOT 1010 (0.53 mm ID; Supelco, Bellefonte,

133 USA) held at 90 °C with a flow rate of ~2.2 mL min^{-1}, and then introduced into the MAT253 Plus IRMS via a Conflo IV

134 interface. Each sample was injected three times during one analysis. The isotopic composition was determined using Isodat

135 3.0 software against the corresponding H_2 working gas (-239‰ for δ^2H) and the values were corrected and normalized using

136 international standards VSMOW2 (0‰ for δ^2H), SLAP2 (-427.5‰ for δ^2H), USGS53 (+40.2‰ for δ^2H) and GFLES-2

137 (159.9‰ for δ^2H). The analytical precision was around 1‰.

138

2.2.3 Carbon ($\delta^{13}C$) substrate analysis

140 Substrates (~100 µg) were weighed into tin capsules (8 × 5 mm, Sercon, Crewe, UK) and placed in a helium-flushed carousel

141 autosampler, then introduced to an Elemental Analyzer IsoLink device (EA IsoLink CNSOH, Thermo Scientific, Bremen,

142 Germany) equipped with a CHN/NC/N EA combustion/reduction reactor (Sercon, Crewe, UK) heated to 1020 °C. A pulse of

143 oxygen was introduced to the reactor simultaneously with the sample. The sample gases were quantified via a thermal

144 conductivity detector (TCD) and then introduced to a MAT 253 Plus isotope ratio mass spectrometer (IRMS; Thermo

145 Scientific; Bremen, Germany) via the open split of a Conflo IV interface, with helium as the carrier gas. The isotopic

146 composition was determined using Isodat 3.0 software against the corresponding CO_2 working gas (-4.191‰ for $\delta^{13}C$), and

147 the values were corrected for linearity and normalized to the VPDB scale using international reference material IAEA-600 (-

148 27.771‰ for $\delta^{13}C$). The analytical precision was <0.04‰.

2.2.3 Pyrolysis GC for lipid analysis

150 The pyrolysis unit Shimadzu 3030D (Shimadzu, Kyoto, Japan/ Frontier Laboratories, Fukushima, Japan) was installed on top

151 of the GC Trace1310 gas chromatograph SSL injector (Thermo Scientific, Bremen, Germany) and the GC was equipped with

152 an SLB-IL60 column (non-bonded; 1,12-Di(tripropylphosphonium)dodecane bis(trifluoromethanesulfonyl)imide phase, 30 m,

153 0.25 mm ID, 0.20 µm df, Supelco, Bellefonte, USA). The furnace temperature was 650 °C and the interface temperature was

154 370 °C. The injector temperature was 360 °C and the GC oven was held at 80 °C for 1 min then ramped to 175 °C at 15 °C

155 min^{-1}, then ramped to 195 °C at 2 °C min^{-1}, then ramped to 300 °C at 10 °C min^{-1}, and finally held at 300 °C for 7 min. Helium

156 was used as the carrier gas, with a constant flow of 1.5 mL min^{-1}, a split ratio of 40, and a split flow of 26.7 mL min^{-1}. The

157 column flow was split via a multichannel device to acquire MS and isotopic data simultaneously from one injection. The

158   GCMS (ISQ QD; Thermo Scientific, Bremen, Germany) ion source was set to electron impact ionization mode (EI) at 70 eV

159   and a scan range of m/z 50 – 500 with a scan time of 0.2 sec^{-1}. Scanning started after 8 min to avoid the solvent peak in the

160   MS. The transfer line temperature was set to 300 °C and the ion source was set to 250 °C.

161   The samples (lyophilized biomass, 0.1 – 1.3 mg) were weighed into an ultra-clean stainless steel Eco-Cup LF (Frontier

162   Laboratories, Fukushima, Japan), which were burned with a torch before usage to remove contaminants. Immediately prior to

163   sample injection, 30 µL of trimethylsulfonium hydroxide (TMSH) was added on the sample to increase the volatization by

164   transforming the fatty acids into fatty acid methyl esters (FAMEs) and improve measurement sensitivity. Identification of

165   FAMEs was performed using fragmentation patterns and the NIST 14 library.

166   Stable C and H isotope compositions of FAMEs from aliquots of the same biomass were separately determined by splitting the

167   flow from the GC column to a GC-IsoLink II reactor, coupled to a MAT253 Plus IRMS via a Conflo IV interface. Values are

168   expressed in standard delta notation ($\delta^{13}C$ and $\delta^{2}H$). MS information was simultaneously acquired by use of the multi-channel

169   device described above. For conversion of FAMEs and ergosterol to CO_2, the combustion reactor (nickel oxide tube with CuO,

170   NiO, and Pt wires) was set to 1000 °C. For conversion of FAMEs and ergosterol to H_2, the pyrolysis reactor (aluminum tube)

171   was set to 1420 °C. The FAMEs were identified by their retention times and fragmentation patterns. The isotopic composition

172   was determined using Isodat 3.0 software against the corresponding CO_2 or H_2 working gas (-4.191‰ for $\delta^{13}C$, -239.5‰ for

173    $\delta^{2}H$). Isotope corrections for instrument drifts, linearity, and normalization to the VPDB or VSMOW scales were performed

174   according to the response of USGS70 (-30.53‰ for $\delta^{13}C$, -183.9‰ for $\delta^{2}H$) and USGS72 (-1.54‰ for $\delta^{13}C$, 348.3‰ for $\delta^{2}H$)

175   reference standards. The analytical precision was < 0.5‰ and < 10‰ for $\delta^{13}C$ and $\delta^{2}H$, respectively.

176

177   **2.3 Calculations**

178   Carbon use efficiency (CUE) for the growth experiments was calculated by normalizing the amount of C in biomass by that

179   plus C that accumulated as CO_2 [CUE = biomass-C / (CO_2-C + biomass-C)]. The $\delta^{13}C$ values of fungal biomarker $C_{18:2}$ was

180   determined as standard delta values (‰). The IC incorporation into the biomarker (%IC) was calculated based on the following

181   equation:

182    $$\%IC_{(assimilation)} = \frac{^{13}F_{lipid} - ^{13}F_{lipid,control}}{^{13}F_{DIC(medium)} - ^{13}F_{substrate}} \times 100 \qquad \textbf{(Eq. 1)}$$

183   **Equation 1: Inorganic carbon (%IC) assimilation was calculated as the difference in the ^{13}C atom fraction of the lipids harvested**

184   **at the end of the labeling experiment ($^{13}F_{lipid}$) compared to the lipids harvested at the end of the natural abundance treatment**

185   **($^{13}F_{lipid,control}$), relative to the difference between the mixing-weighted average ^{13}C atom fraction of dissolved inorganic C ($^{13}F_{DIC}$, cf.**

186   **Text S1) and the ^{13}F of the substrate. F was calculated as $^{13}F = (R^{13/12})/(R^{13/12} + 1)$, where R is re-calculated from the $\delta^{13}C$ ratios**

187   **reported by Isodat Software following measurement by IRMS ($\delta^{13}C = ([R^{13/12}]_{sample}/[R^{13/12}]_{ref} - 1) * 1000$ (modified after Boschker**

188   **& Middelburg 2002; Wegener et al., 2012).**

189   The water H assimilation efficiency (a_w) for fungal biomarker $C_{18:2}$ was approximated from the regressions of the hydrogen

190   isotope composition of individual fatty acids $^2F_{FA}$ and that of medium water ($^2F_{water}$), according to Kopf et al. (2015), after

191   Zhang et al. (2009). Briefly, the hydrogen isotopic compositions of microbial fatty acids produced by an organism generally

192   follow the isotopic composition of environmental water, and are related to the mole fraction of H contributed from water in

193   the cultivation medium (f_W) and the net hydrogen isotope fractionation between fatty acids and water ($\alpha_{fa/w}$), where $a_w = f_w \times$

194    $\alpha_{fa/w}$. Whereas a_W can be determined experimentally, the latter terms cannot be independently determined for heterotrophic

195   growth (Kopf et al., 2015). The traditional isotope effects and $\varepsilon_{C18:2/water}$ and $\alpha_{C18:2/water}$ were calculated after Hayes (2004),

196   where $\alpha_{C18:2/water} = [(\delta^2H_{C18:2} + 1000) / (\delta^2H_{water} + 1000)]$ and $\varepsilon_{C18:2/water} = (\alpha_{C18:2/water} - 1) \times 1000‰$.

197   Notably, calculation of %IC and a_w consider relative increases in $^{13/12}C$ or $^{2/1}H$ composition, and thus do not require a correction

198   for the methyl group added during derivatization of the fatty acid. The $\varepsilon_{C18:2/water}$ values determined in this study were not

199   corrected for the additional methyl group and add an inaccuracy to the reported values, as further discussed below.

200

201   **3 Results**

202

203   **3.1 Fungal growth and CO_2 production**

204   All fungal species were pure cultures, which were incubated in a mineral medium with either glucose, succinate, β-cyclodextrin,

205   or tannic acid serving as the sole organic C source. Growth was monitored by the evolution of CO_2 into the headspace, which

206   ranged from 0.36% (no respiration of substrate) to a maximum of 35%, after incubation times ranging from 5 to 160 days (Fig.

207   1). The pH of the media in all incubations ranged from 2 to 5.5 at the time of harvest, with a general trend of decreasing pH

208   with increasing CO_2; however, the trend was opposite when succinate was the carbon source, with pH increasing from 4 to

209   5.5. For samples that produced sufficient biomass, the dry biomass of harvested fungal hyphae ranged up to 250 mg, and at

210   least 30 μg dry biomass was used to analyze fungal membrane fatty acids by Pyr-GC-IRMS. Only the Ascomycota species PL

211   and PJ grew sufficiently on each tested substrate to produce enough biomass for stable isotope analysis. Incubations of

212   Zygomycota species with glucose or succinate also yielded sufficient dry biomass, and only UM was able to grow on β-

213   cyclodextrin. Zygomycota species produced neither CO_2 nor biomass when incubated with tannic acid. The Basidiomycota

214   typically exhibited the slowest growth, and both species (PI and PC) only produced enough biomass when grown on glucose.

215   The headspace CO_2 levels in Basidiomycota incubations with succinate increased to a maximum of ~ 2%, but only PI yielded

216   sufficient biomass for analysis. PC grew sufficiently on β-cyclodextrin, with CO_2 levels increasing to a maximum of 3%, while

217   CO_2 remained < 0.6% in PI incubations.

218

Glucose

Succinate

Tannic acid

Beta-Cyclodextrin
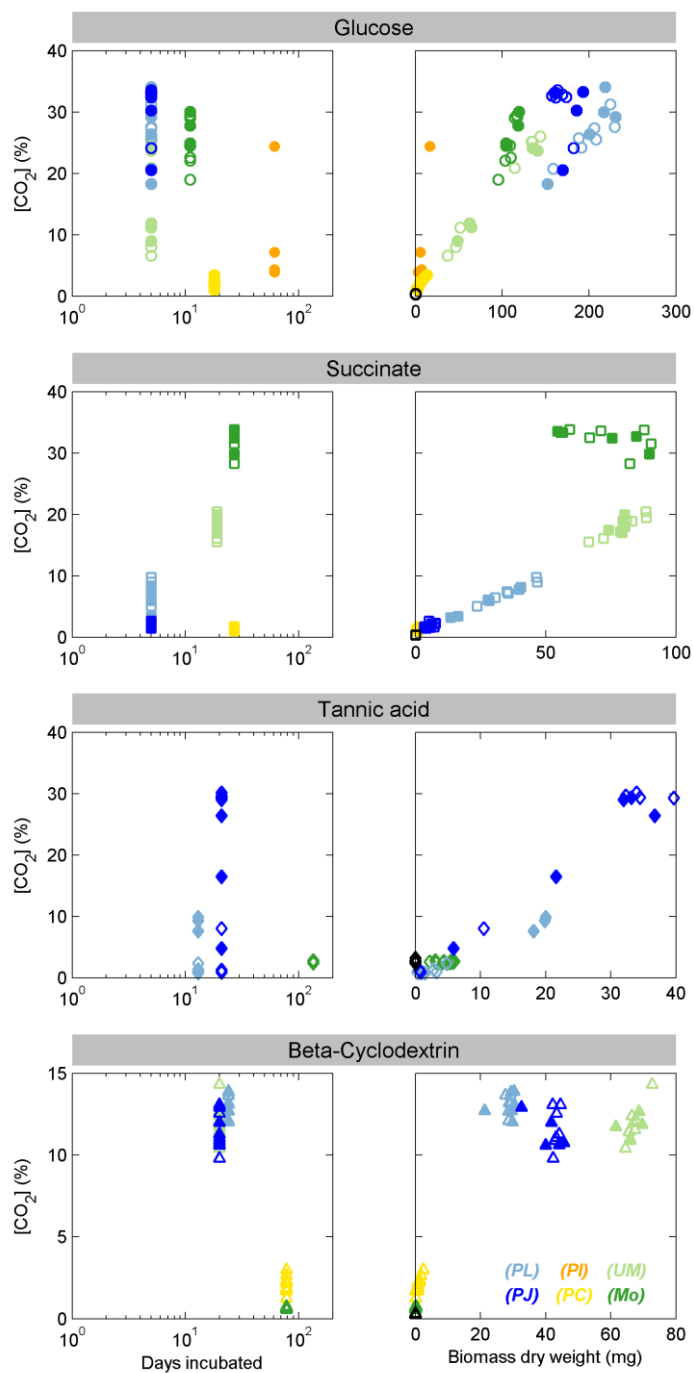
(PL) (PI) (UM)
(PJ) (PC) (Mo)

219

Figure 1. Growth of fungal species on each substrate as indicated by production of CO_2 versus days of incubation (left panels) or dry biomass (right panels). Filled symbols indicate samples for which the $C_{18:2}$ biomarker was measured by Pyr-GC-IRMS. Colors represent the Ascomycota species *Penicillium janczewskii* (PJ, dark blue) and *Paecilomyces lilacinus* (PL, light blue), Zygomycota *Mortierella* sp. (MO, dark green) and *Umbelopsis* sp (UM, light green), and Basidiomycota species *Phanerodontia chrysosporium* (PC, orange) and *Paxillus involutus* (PI, yellow). The symbols denote incubations with glucose (circles), succinate (squares), tannic acid (diamonds), or β-cyclodextrin (triangles).

The growth substrates induced a wide range in CUE values, ranging from 0.1 to 0.6 (Fig. 2). Higher CUE values were typically observed for Ascomycota and Zygomycota species growing on glucose, and lower values for their growth on succinate and tannic acid. CUE estimated for Basidomycota species was always low (< 0.15). The CUE range for growth on glucose (0.1-0.6), β-cyclodextrin (0.1-0.6), and succinate (0.2-0.5) were larger than observed for tannic acid (0.15-0.3).
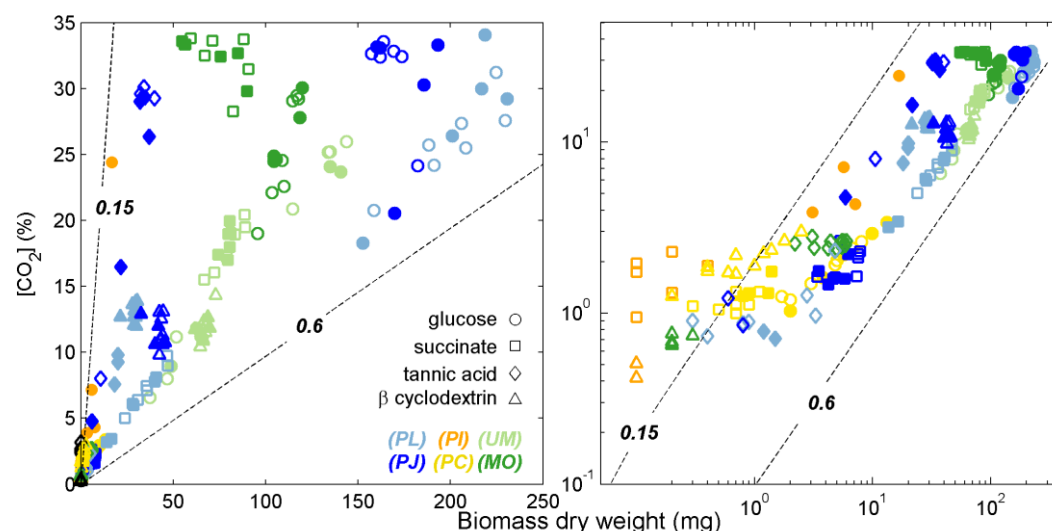
Figure 2. Accumulation of biomass and headspace CO_2 for fungal species from three phyla growing on monomers or complex substrates. The right panel includes the same data on a log-log scale to depict the trends of fungi exhibiting minimal growth. Lines indicate CUE trajectories of 0.15 or 0.6, and were calculated assuming that fungal biomass was 44% C (w/w). Colors and symbols are redundant with Fig. 1. Filled symbols indicate samples that were analyzed by Pyr-GC-IRMS.

3.2 Stable isotopic composition of fungal lipids

Fungal respiration of the different (unlabeled) growth substrates led to decreasing $\delta^{13}C$-CO_2 values as fungal biomass was produced, which followed a hyperbolic trend expected for the mixing of CO_2 from two different sources (Text S1; c.f., Kendall

and Caldwell, 1998). The atom % ^{13}C in control incubations with no fungal inoculum was measured at the latest time of harvest of inoculated incubations and stayed below 0.4%, except for incubations with tannic acid, where it ranged between 2% and 3%; the $\delta^{13}C$ values of the substrates were glucose = -26.5‰; succinate = -28.3‰, tannic acid = -27.4‰, β-cyclodextrin = -10.6‰. The mixing relationship was modeled using all CO_2 data, across all incubations, and integrated to approximate the mixing-weighted average ^{13}F value of IC for each incubation (cf., Text S1, Fig. S2), which was finally applied in the denominator of Eq. 1 to estimate the fraction of lipid-C derived from IC. For incubations that produced sufficient fungal biomass for stable C isotopic analysis, the weighted average $\delta^{13}C$ values of IC that were applied in Eq. 1 ranged from 200 to 1400 ‰ (i.e., ~ 1.3 to 2.6 AT% ^{13}C), and was largely dependent on how much of the substrate was respired to CO_2.

3.2.1 Carbon isotopes

The $\delta^{13}C$ values of fungal biomarker fatty acid $C_{18:2}$ (Table 1) produced under natural cultivation conditions with glucose (i.e., non-labeled; AT%$_{DIC}$ ~ 1%) ranged from -24.1‰ to -21.2‰ across all strains (n = 6 species). As expected, $C_{18:2}$ harvested from the labeled incubations exhibited slightly higher $\delta^{13}C$ values (up to +11‰; PC grown on glucose) than the corresponding experiment amended with natural bicarbonate, likely owing to the incorporation of labeled IC into the $C_{18:2}$ fatty acid.

Table 1: $\delta^{13}C$ values of fungal biomarker $C_{18:2}$ harvested from incubations with non-labeled substrates (nat) or those amended with ^{13}C-labeled bicarbonate. Incorporation of inorganic C (%IC) was calculated based on Eq.1. Errors represent the standard deviation of replicate incubations. Not all fungal species grew sufficiently on all substrates and thus %IC could not have been determined (n.d).

Species	Glucose $\delta^{13}C$ (‰)		IC (%)	Succinate $\delta^{13}C$ (‰)		IC (%)	Tannic acid $\delta^{13}C$ (‰)		IC (%)	β-cyclodextrin $\delta^{13}C$ (‰)		IC (%)
	nat	+		nat	+		nat	+		nat	+	
Paxillus involutus (PI)	-21.5	-16.7	0.6 (±0.2)	n.d	n.d	n.d	n.d	n.d	n.d	n.d	n.d	n.d
Phanerodontia chrysosporium (PC)	-24.1	-15.9	0.9 (±0.3)	-27.3	-23.5	0.3 (±0.1)	n.d	n.d	n.d	n.d	n.d	n.d
Mortierella (MO)	-21.9	-20.7	0.5 (±0.1)	-31.7	-31.5	0.1 (±0.1)	n.d	n.d	n.d	n.d	n.d	n.d
Umbelopsis (UM)	-21.2	-21.1	0.1 (±0.0)	-30.6	-28.2	0.7 (±0.2)	n.d	n.d	n.d	-21.7	-18.1	0.8 (±0.3)
Penicillium janczewskii (PJ)	-23.2	-22.1	0.5 (±0.2)	-30.1	-27.8	0.2 (±0.0)	-25.9	-20.5	2.2 (±0.5)	-20.7	-20.1	0.1 (±0.2)
Paecilomyces lilacinus (PL)	-23.0	-23.5	n.d	-30.8	-29.9	0.1 (±0.0)	-25.4	-25.0	0.1 (±0.0)	-19.1	-17.6	0.7 (±0.4)

The estimated incorporation of IC into $C_{18:2}$ (%IC) typically ranged up to 1%; only PJ grown on tannic acid exhibited higher %IC values, which ranged up to 2.2% (Table 1, Fig. 3). There were no general trends observed in %IC with other measured or estimated parameters, including CUE; however, for the two species that were able to grow on tannic acid, %IC was positively correlated with the amount of CO_2 and biomass produced during the incubation ($R^2 > 0.85$, n = 5, $p < 0.01$).
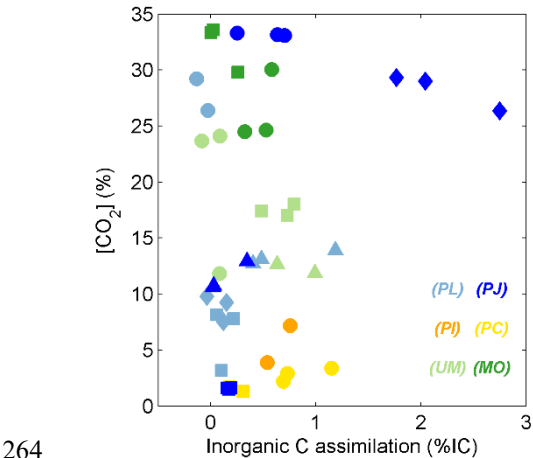
Figure 3. %IC values for fungal species respiring glucose (circles), succinate (squares), tannic acid (diamonds), or β-cyclodextrin (triangles). Colors represent individual fungal isolates as described in Fig. 1.

3.2.2 Water assimilation factor (a_w)

The "net" contribution of water hydrogen to lipid H is reported as the water hydrogen assimilation factor a_w (Kopf et al., 2015), and was estimated based on the slope of the linear regression line between H isotopic composition of lipid versus growth medium water (Fig. 4), which ranged from natural MilliQ (δ^2H = -45‰ ± 10‰) to the labeled treatments (65‰ ± 4‰; 166‰ ± 10‰; 368‰ ± 27‰). The a_w values for the fungal biomarker $C_{18:2}$ grown on glucose ranged from 0.37 ± 0.03 to 0.75 ± 0.06 with an average value of 0.60 ± 0.05 (n = 6 species; ±SEM). When grown on succinic acid, the a_w values for $C_{18:2}$ harvested from individual species ranged from 0.78 ± 0.01 to 0.96 ± 0.02 with an average value of 0.83 ± 0.04 (n = 4 species; ±SEM). When grown on tannic acid, the a_w values for $C_{18:2}$ harvested from individual species ranged from 0.74 ± 0.06 to 0.77 ± 0.03, and when grown on β-cyclodextrin the a_w values for $C_{18:2}$ ranged from 0.46 ± 0.03 to 0.68 ± 0.04 with an average value of 0.58 ± 0.06 (n = 4 species; ±SEM). The average a_w values for $C_{18:2}$ for all substrates and species was 0.67 ± 0.04 (±SEM).

3.2.3 H isotope fractionation factors $\alpha_{C18:2/water}$ and $\varepsilon_{C18:2/water}$

281 The range of traditionally reported isotope effects $\alpha_{C18:2/water}$ and $\varepsilon_{C18:2/water}$ (Sessions and Hayes, 2005) for all natural and ^{2}H-
282 labeled fungal growth experiments was 0.73 to 1.08 and -265 to +83 ‰, respectively (Table S1). PL growth on tannic acid
283 exhibited the highest values (0.97 to 1.08 and -35 to +83 ‰, respectively; Fig. 5, Table S1), while for all other growth
284 experiments, $\alpha_{C18:2/water}$ and $\varepsilon_{C18:2/water}$ remained < 0.94 and -65 ‰, respectively. Considering only the growth experiments
285 performed without label addition, the average (±SD) $\varepsilon_{C18:2/water}$ values were not significantly different for fungi growing on
286 glucose (-115 ± 34 ‰, n = 13), succinate (-111 ± 35 ‰, n = 8), or β-cyclodextrin (-133 ± 7‰, n = 6), but growth on tannic
287 acid elicited significantly higher values (+12 ± 81 ‰, n = 5; $p < 0.01$, two-tailed homoscedastic t-test), Within species
288 comparisons revealed that both Zygomycota species (*Mortierella* and *Umbelopsis*) exhibited significantly more negative
289 $\varepsilon_{C18:2/water}$ values when grown on succinate (-127±6 and -155±8 ‰, n = 2) versus glucose (-78±3 and -127±5 ‰, respectively,
290 n = 2; $p < 0.05$). The only other significant differences in $\varepsilon_{C18:2/water}$ values were observed for growth of the Ascomycota species
291 *P. lilanicus*, for which growth on tannic acid (+71±18 ‰, n = 3) yielded higher values than on glucose (-122±15 ‰, n = 2),
292 succinate (-84±6 ‰, n = 2), and β-cyclodextrin (-132±2 ‰, n = 2; all $p < 0.01$); the $\varepsilon_{C18:2/water}$ values for growth on succinate
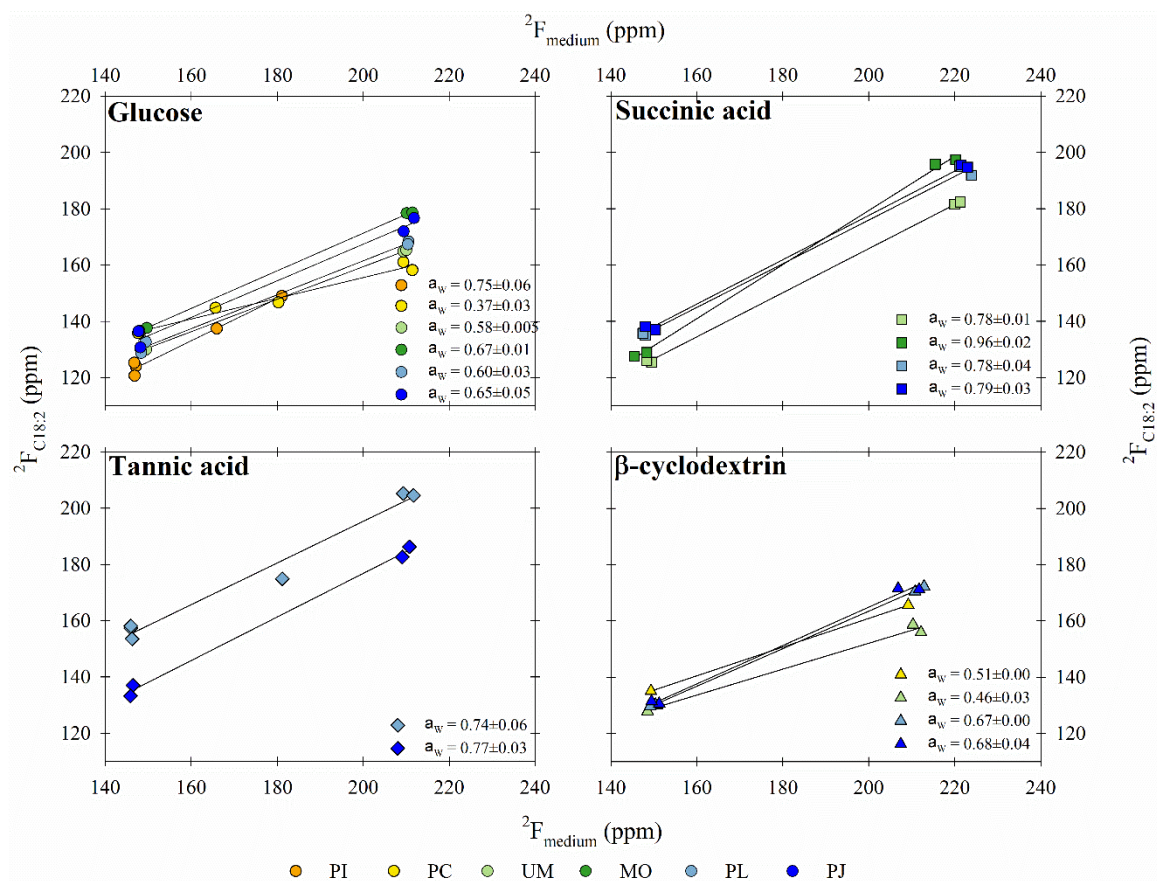293 and β-cyclodextrin were also significantly different ($p < 0.01$).

294

295

Figure 4. The water hydrogen assimilation factor (a_w values) estimated as the slope of the fractional [2/1]H abundance ([2]F) in lipids (y-axis) versus medium water (x-axis). Data are shown for fungal biomarker $C_{18:2}$ produced during growth on the different substrates (glucose, succinic acid, tannic acid and β-cyclodextrin) and harvested from the different fungal isolates *[Paxillus involutus* (PI), *Phanerodontia chrysosporium* (PC), *Mortierella* sp. (MO), *Umbelopsis* sp. (UM), *Penicillium janczewskii* (PJ), and *Paecilomyces lilacinus* (PL)]. R^2 values for all slopes were > 0.97.
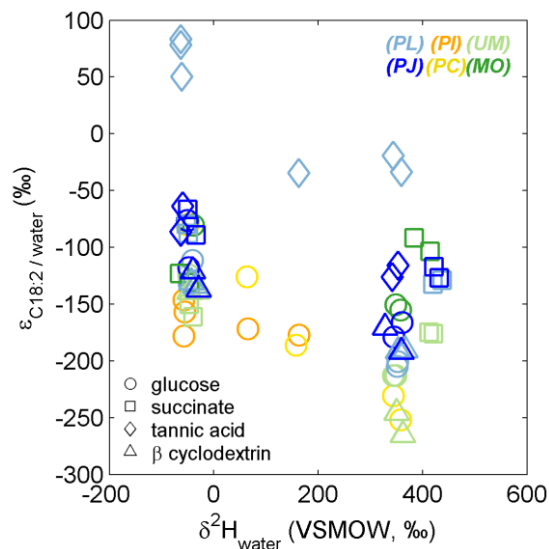
Figure 5. The apparent isotope effect ($\varepsilon_{C18:2/water}$) for fungi grown in medium having variable δ^2H_{water} composition. The colors and symbols are redundant with Fig. 1. For each species-substrate pair, the large range and/or decrease in $\varepsilon_{C18:2/water}$ in ^{2}H-enriched medium are expected, given the additional contributions of substrate-H and metabolic water-H to lipid-H during biosynthesis.

4 Discussion

4.1 Fungal growth dynamics

Collectively, the fungal incubation experiments included six species representing three different phyla growing on one of four substrates, and exhibited a large range in the relative amounts of CO_2 (0.2-34% v/v) and biomass produced (0-230 mg dry weight; Fig. 1), with CUE ranging from 0.15 to 0.6 (Fig. 2). While atmospheric, oxic conditions likely prevailed during most of the incubation period, it is probable that some incubations turned anoxic when CO_2 levels exceeded 21%, which occurred in incubations of Ascomycota and Zygomycota growing on glucose, Ascomycota growing on tannic acid, and Zygomycota growing on succinate. The accumulation of CO_2 was necessary consequence of performing the incubations in closed bottles, which was required to prevent the escape of ^{13}C-labeled IC and also to prevent microbial contaminations. Nevertheless, such alteration between oxic and anoxic conditions is common in natural environments, and the measured IC assimilation into fungal lipids was consistently low (< 3%; Fig. 3), regardless the implied anoxia. Furthermore, the observed variability in CUE, %IC, and a_w between growth experiments were not correlated with large increases in headspace CO_2.

4.2 Fungal IC assimilation into lipids

A fundamental process in nature and basis for ecological food webs is the fixation of IC via photosynthesis and/or chemosynthesis by autotrophic organisms. The IC assimilation by heterotrophic organisms also plays an important role in ensuring the provision of energy and to replenish intermediates in the TCA cycle that have been released for biosynthesis (Kornberg 1965). Therefore, IC assimilation is a proxy for both anabolic processes and the catabolic status of the cell, influenced by assimilation, biosynthesis, anaplerotic reactions, and redox balancing reactions (Braun et al., 2021; Erb 2011). Previous reports on the by-fixation of IC (%IC) via anaplerotic pathways into heterotrophic biomass varied between 1% and 8% (Dijkhuizen & Harder, 1985; Feisthauer et al., 2008; Romanenko 1964; Roslev et al., 2004), whereas for fungi it was previously reported to amount to roughly 1% (Sorokin 1961; Schinner & Concin, 1981; Schinner et al., 1982), and was recently shown to vary between 2% and 12% for Ascomycota when grown on glucose or glutamic acid (Jabinski et al., 2024). Our results, focusing on a specific fatty acid biomarker, demonstrate a low range in %IC for all different substrates and species tested in this study (0 - 3%), with the Ascomycota (0 - 2%) assimilating relatively less IC than previously reported species (4.6% ± 1.6%; Jabinski et al., 2024). The highest observed incorporation was 2.2 ± 0.5% by *Penicillium janczewskii* (PJ, n = 3) when grown for 21 days on tannic acid (Table 1; Fig. 3). Only the other Ascomycota species, *Paecilomyces lilacinus* (PL), grew sufficiently on tannic acid (up to 10% CO_2 and 20 mg dry weight after 13 days; %IC = 0.14 ± 0.02%, n = 3 ; Figs. 1, 3), suggesting that increased assimilation of IC by PJ may have occurred during the extra week of incubation and promoted higher biomass production. The high CO_2 levels also suggest that the incubations of PJ with tannic acid may have turned anoxic, which may also explain the higher IC incorporation in these incubations. Overall, heterotrophic IC assimilation does not appear to be a hallmark of any of the variety of fungal taxa or catabolic pathways probed in this study.

4.3 Water hydrogen incorporation into fungal lipid biomarker $C_{18:2}$

As demonstrated previously, the regression slope between hydrogen isotopic composition of water medium and microbial lipids (i.e., a_w) varies with the type of metabolism (Zhang et al., 2009; Valentine, 2009; Wijker et al., 2019; Jabinski et al., 2024), and importantly for heterotrophs, a non-negligible proportion of hydrogen may derive from sources other than ambient water. For fatty acid biosynthesis, H incorporation is suggested to be a function of transporters and electron acceptors (NADPH and NADH), with contributions accounting for around half of all lipid hydrogen (Maloney et al., 2024). The remaining comprises equal contributions of H obtained directly from environmental water or acetyl-CoA (Valentine, 2009; Zhang et al., 2009; Caro et al., 2023). The consensus from previous studies that investigated the lipids of heterotrophic bacteria is that microbial heterotrophs exhibit a_w values ranging from 0 to 1, with a mean of 0.71±0.17 (e.g., Caro et al., 2023), though some organisms have exhibited a_w values exceeding 1 (Dirghangi et al., 2013; Jabinski et al., 2024). Jabinski et al. (2024) demonstrated that five species of heterotrophic Ascomycota exhibit similar a_w values (0.62 ± 0.04) for the fungal biomarker $C_{18:2}$ during growth on glucose. Zhang et al. (2009) reported similar a_w values for *E.coli* grown on glucose (0.63 ± 0.03). In the current study, a_w values for the fungal biomarker $C_{18:2}$ during growth on glucose (0.60 ± 0.05) were agreeable with Jabinski et al. (2024), but more variable, likely owing to the broader phylogenetic coverage of the current study.

359   The large variability in $\varepsilon_{C18:2/water}$ estimates (Fig. 5; Table S1) can be partly attributed to the large range in δ^2H of medium water,

360   which contributes H together with the substrate and metabolic water to determine $\delta^2H_{C18:2}$, even though the net isotope effect

361   ($\alpha_{C18:2/water}$) may be consistent for a specific species-substrate pair (Session and Hayes, 2005; Kopf et al., 2015). In other words,

362    $\varepsilon_{C18:2/water}$ values do not account for the admixture of H sources that also affect $\delta^2H_{C18:2}$ of heterotrophic fungi. More robust

363   differences were observed in a_w values both between and within the different phyla and substrates tested.

364

365   *4.3.1 Trends across fungal phyla*

366   For incubations in which the Zygomycota isolates produced enough biomass to determine a_w (i.e., glucose, succinate, β-

367   cyclodextrin; $n = 5$; Fig. 4), we observed a highly significant inverse correlation with CUE ($R^2 = 0.87$, p < 0.01; Fig. 6),

368   suggesting coupling of a_w with growth efficiency. Presumably, the proportion of substrate-derived H incorporated into lipids

369   increases with more efficient incorporation of substrate C into biomass. Ascomycota exhibited the most consistent a_w values

370   among phyla when grown on each of the four different substrates [0.63 ± 0.03 (glucose); 0.78 ± 0.01 (succinate); 0.76 ± 0.02

371   (tannic acid); 0.67 ± 0.01 (β-cyclodextrin)], but also the largest variability in CUE (0.08-0.59; Fig. 2). CUE and a_w exhibited a

372   similar trend as observed for Zygomycota isolates, but were not significantly correlated across incubations of Ascomycota,

373   Basidiomycota only produced sufficient biomass when fed substrates that activated the glycolytic pathway (glucose or β-

374   cyclodextrin; CUE < 0.3), yet showed high variability in a_w between species ($0.37 \pm 0.03 < a_w < 0.75 \pm 0.06$; Fig. 4), which

375   were beyond the more confined range of a_w values determined for isolates belonging to Zygomycota and Ascomycota.

376
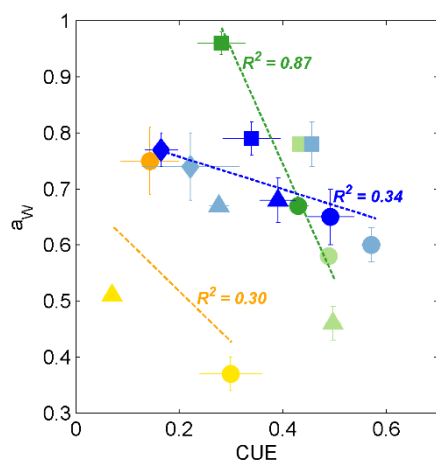
377

378   **Figure 6. Biplot of CUE and a_w values for fungi growing on glucose (circles), succinate (squares), tannic acid (diamonds),**

379   **or β-cyclodextrin (triangles). The colors are redundant with Fig. 1, representing the phlya Ascomycota (blue shades, *n***

380   **= 8), Zygomycota (green shades, *n* = 5), and Basidiomycota (yellow and orange symbols, *n* = 3). The dashed lines and**

381   **R^2 values indicate the linear regression for the corresponding phylum across all substrates that yielded sufficient**

382   **biomass. Only the regression for Zygomycota was significant (p < 0.01).**

383

4.3.1 Trends across C substrates

Across all incubations, the similar a_w values determined for growth on glucose (0.60 ± 0.05) versus β-cyclodextrin (0.58 ± 0.06), of which the latter consists of seven glucopyranose units ($C_6H_{12}O_6$), suggests that the catabolism of glucose subunits via glycolysis overprints signals of water-H incorporation that may derive during degradation of the β-cyclodextrin oligomer. Alternatively to glycolysis, succinate yielded significantly higher a_w values (0.83 ± 0.05), which was in the same range as reported for *C. oxalaticus* when grown on succinate (a_w 0.80 ± 0.05; Zhang et al., 2009), and was more similar to that reported previously for fungal growth on glutamic acid (0.90 ± 0.07; Jabinski et al., 2024). Considering all fungal incubations, a one-way analysis of variance (ANOVA; Holm-Sidak method; SigmaPlot v11) confirmed the significant difference in a_w values between growth on glucose and glutamic acid ($p < 0.001$), glutamic acid and β-cyclodextrin ($p < 0.001$), succinate and glucose ($p < 0.003$), and succinate and β-cyclodextrin ($p < 0.005$). It also confirmed that there was no significant difference between the other substrate combinations ($p > 0.05$).

Glutamic acid and succinate are thought to be introduced into the TCA cycle through coupled metabolites, where succinate is a direct metabolite of the TCA cycle and glutamic acid is converted to α-ketoglutarate by transamination before entering the TCA cycle, which is only 2 steps from succinate (Cooper et al., 2014). Also, being acids, these substrates may have a greater capacity than saccharides to exchange H with ambient water at experimental pH (typically $2 < pH < 5.2$), especially glutamic acid, which also comprises an amino moiety. Tannic acid (0.76 ± 0.02) yielded no significant differences ($p > 0.05$) from the other substrates, and is reported to be degraded to different subunits including gallic acid and glucose (Banerjee and Mahapatra, 2012; Lekha and Lonsane, 1997 and references within). Aromatic degradation pathways employed by fungi generate intermediates that go through the β-ketoadipate pathway (Mäkelä et al., 2015) before entering the TCA cycle as a succinyl-CoA metabolite (Lekha and Lonsane, 1997). The a_w values induced by degradation of tannic acid suggest that it integrates both the lower a_w signature of glycolysis and higher a_w signature of the TCA cycle (Fig. 7).

Together, our incubation experiments suggest that a_w values determined for the fungal biomarker $C_{18:2}$ could not distinguish between fungal growth on relatively labile monomers (i.e., glucose and succinate; requiring as few as 5 days of cultivation) versus larger, less-labile substrates (i.e., β-cyclodextrin and tannic acid; requiring 20 to 183 days of cultivation). However, a_w values of fungal lipid biomarkers may be indicative of fungi employing primarily glycolytic or TCA pathways. Environmental assays that quantify fungal lipid production via the incorporation of ambient water-H (i.e., the lipid-SIP approach) may upscale to total production estimates by applying our calculated mean a_w value of 0.69 ± 0.03 [n = 27; ± (SEM)], which is consistent with the a_w value of 0.71 recommended for soil microbial communities (Caro et al., 2023). For [2]H-SIP investigation of fungal ecotypes supplied with TCA metabolites, such as mycorrhiza, the a_w value of $C_{18:2}$ may range up to 0.83 ± 0.05. Similar approaches could be applied to environmental samples, such that the a_w values of phospholipids containing C18:2 fatty acids could inform the distribution of predominant metabolic ecotypes across a soil profile.

415   Comparisons of net $^{2/1}$H fractionation factors (i.e., $\varepsilon_{18:2/H2O}$; Table S1) estimated in the current study to previous reports are

416   most relevant for those derived from our natural abundance incubations. However, we note that these estimates were

417   determined for a fewer number of replicates (n = 2 or 3) and represent the distinct value relative to our laboratory water (δ^2H

418   = -49 ‰), which varies from labeled treatments (Table S1) and likely natural systems having a significantly different δ^2H_{H2O}.

419   Fungal isolates that could successfully grow on tannic acid exhibited the highest $^2\varepsilon_{18:2/H2O}$ values, which is likely manifested

420   by NADPH production and turnover (e.g. Wijker et al., 2019). The Zygomycota isolates investigated in the current study

421   (*Mortierella* and *Umbelopsis*) both exhibited relatively strong fractionation of $^{2/1}H_{water}$ during growth on succinate ($\varepsilon_{18:2/H2O} <$

422   -123 ‰), which contrasts the trends observed for Ascomycota isolates and previous reports of heterotrophic bacteria (e.g.,

423   Zhang et al., 2009), where $\varepsilon_{18:2/H2O}$ values are typically higher for succinate relative to other C substrates. Together, the relatively

424   strong $^{2/1}$H fractionation (i.e., low $\varepsilon_{18:2/H2O}$) and high water isotope incorporation efficiency (a_w) suggest these Zygomycota

425   isolates employ an alternative catabolic pathway for succinate, resulting in minor incorporation of succinate-derived H into

426    $C_{18:2}$.

427

428   **4.4 Dual-SIP approach**

429

430   Dual-SIP experiments with ^2H_2O and ^{13}C-dissolved IC previously highlighted the potential to track microbial activity and

431   distinguish heterotopic vs autotrophic metabolic modes within environmental settings and pure cultures (Kellerman et al.,

432   2012, 2016; Wegener et al., 2012; Huguet et al., 2017; Wu et al., 2018, 2020). This approach was also previously applied to

433   investigate fungal pure cultures (Jabinski et al., 2024), in which the plot of assimilation of IC versus water-H into the fungal

434   biomarker $C_{18:2}$ could distinguish five Ascomycota species growing on glucose or glutamic acid, with a_w values explaining

435   most of the variability. While calculated IC:a_w are useful to distinguish autotrophic from heterotrophic growth (cf. Wegener et

436   al., 2016), all calculated values in this study remained near zero, with %IC ranging up to 3% and a_w values ranging from 0.37

437   to 0.96 (Fig. 4). This pure culture study therefore suggests that fungal assimilation of IC is low and less insightful than the

438   more distinguishable a_w values for identifying the relative contributions of fungal phylotypes or ecotypes in environmental
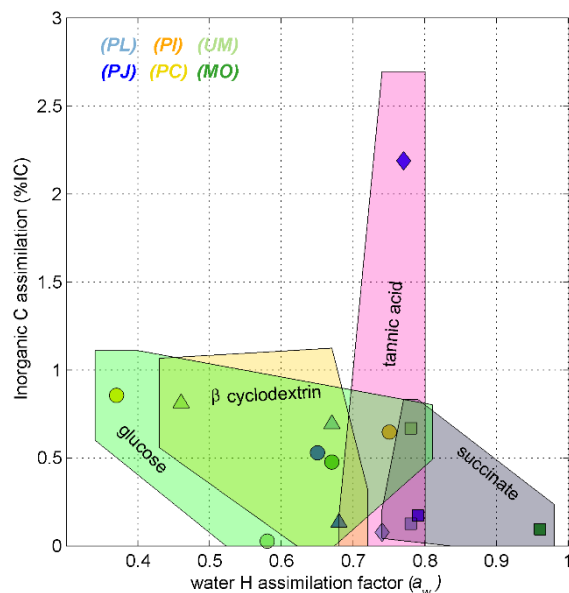
439   assays.

Figure 7. Scatterplot of %IC and a_w values plot for $C_{18:2}$ harvested from incubations of Ascomycota (blue symbols), Basidiomycota (yellow and orange symbols), and Zygomycota (green symbols). The shaded polygons span the range of %IC and a_w values (± propagated error) for fungal growth on glucose (circles, green shape), succinate (squares, grey shape), tannic acid (diamonds, pink shape), or β-cyclodextrin (triangles, yellow shape). Each data point represents one species-substrate pair determined for $n > 4$ growth experiments.

5 Conclusion

The purpose of this work was to apply the dual-SIP assay on pure fungal cultures to define the effect of different organic C substrates on the incorporation of water-H and IC into their membrane lipids. Although heterotrophic CO_2 fixation by microbes may range up to 8% of biomass C, the IC assimilation into the fungal biomarker $C_{18:2}$ harvested from six species representing Ascomycota, Basidiomycota, and Zygomycota did not vary consistently between species or substrate, and remained below 3%. Our findings suggest that the fungal catabolic pathways activated by the variety of substrates tested in this study cannot fully account for the higher levels of heterotrophic CO_2 incorporation reported in natural systems. However, *Penicillium janczewskii*, the species that was most successful at respiring tannic acid, also exhibited the highest %IC value of all incubations (Fig. 3; Fig. 7), suggesting that fungal degradation of similarly complex substrates may rely in part on the assimilation of IC (e.g., via anaplerotic reactions). The use of SIP to estimate %IC of heterotrophs required (*i*) a closed system to prevent loss of ^{13}C label to the atmosphere, and (*ii*) a high label dose, to contend with the accumulation of CO_2 respired from growth substrate.

458 These conditions intensified upon decreases in pH during the growth experiments, thereby shifting the speciation of IC toward

459 CO_2, which may have further, yet unknown consequences for anaplerotic incorporation of the IC. Future applications to

460 determine %IC for microbial heterotrophs should consider repeated spiking or continuous cultivation practices to better

461 stabilize pH and $\delta^{13}C_{DIC}$. Likewise, it would be worth considering isotopic analyses of other potential bioindicator compounds

462 (e.g., sterols, peptides, aminosugars) to see whether incorporation of the IC into such other compounds would render higher

463 levels than fatty acids.

464 In contrast to %IC, we conclude that substrates that activated the glycolysis pathway yielded significantly lower a_w values

465 than those catabolized as TCA intermediates. The relatively high $\varepsilon_{18:2/H2O}$ values harvested from fungi grown on tannic acid

466 may further help to distinguish fungal ecotypes growing on complex, aromatic-containing substrates in natural systems. The

467 expanded a_w dataset reported in this study suggests that the accuracy of fungal production estimated by ^{2}H-lipid SIP

468 experiments can be improved by applying the average a_w value of 0.69 for saprotrophic fungi or up to 0.83 for mycorrhizal

469 fungi. Furthermore, determination of a_w values in environmental ^{2}H-SIP assays may be useful to identify the relative

470 contributions of fungal ecotypes that rely on C substrates fueling glycolysis (e.g., leaf litter) versus those that are fed

471 primarily by TCA intermediates (e.g., root or microbial exudates). Lastly, to our knowledge, the two Zygomycota strains

472 investigated in this study provide the first evidence of a potential correlation between a_w and CUE (Fig. 6), encouraging

473 further exploration of the link between these two parameters, both of which are coupled to microbial central metabolic

474 pathways.

475

476 **Data availability**

477 Data presented in the figures and tables are available in supplementary material (Table S1) and will be made available on the

478 Fractome Database (https://fractome.caltech.edu/).

479

480 **Author contribution**

481 SJ, Conceptualization, Data curation, Formal analysis, Investigation, Methodology, Software, Validation,

482 Visualization, Writing – original draft, Writing – review and editing

483 VK, Investigation, Methodology, Resources, Writing – review and editing

484 MK, Formal analysis, Methodology, Resources, Validation,

485 JJ, Conceptualization, Formal analysis, Methodology, Resources, Validation, Writing – review and editing

486 TBM, Conceptualization, Data curation, Formal analysis, Funding acquisition, Investigation, Methodology, Project

487 administration, Resources, Software, Supervision, Validation, Visualization, Writing – original draft, Writing – review and

488 editing

489

490 **Competing interests**

491 The authors declare that they have no conflict of interest.

492 **Disclaimer Acknowledgements**

502

503
504
505
506

References

Baldrian, P., Voříšková, J., Dobiášová, P., Merhautová, V., Lisá, L., & Valášková, V. Production of extracellular enzymes and degradation of biopolymers by saprotrophic microfungi from the upper layers of forest soil. *Plant and Soil,* 338(1-2), 111-125. doi:10.1007/s11104-010-0324-3, 2011.

Banerjee, D., & Mahapatra, S. Fungal tannase: a journey from strain isolation to enzyme applications. *Dyn Biochem Process Biotechnol Mol Biol,* 6(2), 49-60, 2012.

Boer, W. D., Folman, L. B., Summerbell, R. C., & Boddy, L. Living in a fungal world: impact of fungi on soil bacterial niche development. *FEMS microbiology reviews,* 29(4), 795-811, 2005.

Boschker HTS, Middelburg JJ. Stable isotopes and biomarkers in microbial ecology. *FEMS Microbiol Ecol* 40:85–95. https://doi.org/10. 1111/j.1574-6941.2002.tb00940.x 2002.

Boschker, H. T. S., Nold, S. C., Wellsbury, P., Bos, D., De Graaf, W., Pel, R., ... & Cappenberg, T. E. . Direct linking of microbial populations to specific biogeochemical processes by 13C-labelling of biomarkers. *Nature,* 392(6678), 801-805, 1998.

Braun A, Spona-Friedl M, Avramov M, Elsner M, Baltar F, Reinthaler T, Herndl GJ, Griebler C. Reviews and syntheses: heterotrophic fixation of inorganic carbon–significant but invisible flux in environmental carbon cycling. *Biogeosciences* 18:3689–3700. https://doi.org/10. 5194/bg-18-3689-2021, 2021.

Bukovská P, Bonkowski M, Konvalinková T, Beskid O, Hujslová M, Püschel D. Utilization of organic nitrogen by arbuscular mycorrhizal fungi-is there a specific role for protists and ammonia oxidizers? Mycorrhiza. ;28(3):269–83. https://doi.org/10.1007/s00572-018-0825-0, 2018.

Canarini, A., Fuchslueger, L., Schnecker, J., Metze, D., Nelson, D. B., Kahmen, A., ... & Richter, A. Soil fungi remain active and invest in storage compounds during drought independent of future climate conditions. *Nature Communications*, *15*(1), 10410, 2024.

Carlson C.A., N.R. Bates, D.A. Hansell, D.K. Steinberg. Carbon Cycle. In: J. Steele, S. Thorpe, K. Turekian (Eds.) Encyclopedia of Ocean Science, 2nd Edition. Academic Press, 477-486, 2001.

Caro, T. A., McFarlin, J., Jech, S., Fierer, N., & Kopf, S. Hydrogen stable isotope probing of lipids demonstrates slow rates of microbial growth in soil. Proceedings of the National Academy of Sciences, 120(16), e2211625120, 2023.

Ciais, P., Dolman, A. J., Bombelli, A., Duren, R., Peregon, A., Rayner, P. J., . . . Marland, G. Current systematic carbon-cycle observations and the need for implementing a policy-relevant carbon observing system. Biogeosciences, 11(13), 3547-3602. doi:10.5194/bg-11-3547-2014, 2014.

Cooper AJL, Kuhara T. α-Ketoglutaramate: an overlooked metabolite of glutamine and a biomarker for hepatic encephalopathy and inborn errors of the urea cycle. Metab Brain Dis 29:991–1006. https:/ /doi.org/10.1007/s11011-013-9444-9, 2014.

539 Dijkhuizen, L., & Harder, W. Microbial metabolism of carbon dioxide. Comprehensive biotechnology: the principles,
540 applications, and regulations of biotechnology in industry, agriculture, and medicine/editor-in-chief, Murray Moo-Young,
541 1985.

542 Dumont, M. G., & Murrell, J. C. Stable isotope probing—linking microbial identity to function. Nature Reviews Microbiology,
543 3(6), 499-504, 2005.

544 Erb TJ. Carboxylases in natural and synthetic microbial pathways. Appl Environ Microbiol 77:8466–8477.
545 https://doi.org/10.1128/AEM. 05702-11, 2011.

546 Feisthauer, S., Wick, L. Y., Kästner, M., Kaschabek, S. R., Schlömann, M., & Richnow, H. H. Differences of heterotrophic
547 13CO2 assimilation by Pseudomonas knackmussii strain B13 and Rhodococcus opacus 1CP and potential impact on biomarker
548 stable isotope probing. Environmental Microbiology, 10(6), 1641-1651, 2008.

549 Fioretto, A., Di Nardo, C., Papa, S., & Fuggi, A. Lignin and cellulose degradation and nitrogen dynamics during decomposition
550 of three leaf litter species in a Mediterranean ecosystem. Soil Biology and Biochemistry, 37(6), 1083-1091.
551 doi:10.1016/j.soilbio.2004.11.007, 2005.

552 Fischer, C. R., Bowen, B. P., Pan, C., Northen, T. R., & Banfield, J. F. Stable-isotope probing reveals that hydrogen isotope
553 fractionation in proteins and lipids in a microbial community are different and species-specific. ACS chemical biology, 8(8),
554 1755-1763, 2013.

555 Frey, S. D. Mycorrhizal fungi as mediators of soil organic matter dynamics. Annual review of ecology, evolution, and
556 systematics, 50, 237-259. doi:10.1146/annurev-ecolsys-110617-062331, 2019.

557 Grinhut, T., Hadar, Y., & Chen, Y. Degradation and transformation of humic substances by saprotrophic fungi: processes and
558 mechanisms. Fungal biology reviews, 21(4), 179-189, 2007.

559 Hayes, J. M. An introduction to isotopic calculations. Woods Hole Oceanographic Institution, Woods Hole, MA, 2543, 2004.

560 Hoefs, J. Stable isotope geochemistry. Springer International Publishing AG, part of Springer Nature. doi:10.1007/9783-319-
561 78527-1, 2018.

562 HoÈgberg, P., Nordgren, A., Buchmann, N., Taylor, A. F., Ekblad, A., HoÈgberg, M. N., . . . Read, D. J. Large-scale forest
563 girdling shows that current photosynthesis drives soil respiration. Nature, 411(6839), 789-792, 2001.

564 Huguet, A., Meador, T. B., Laggoun-Défarge, F., Könneke, M., Wu, W., Derenne, S., & Hinrichs, K.-U. Production rates of
565 bacterial tetraether lipids and fatty acids in peatland under varying oxygen concentrations. Geochimica et
566 Cosmochimica Acta, 203, 103-116. doi:10.1016/j.gca.2017.01.012, 2017.

567 Jabinski, S., d. M. Rangel, W., Kopáček, M., Jílková, V., Jansa, J., & Meador, T. B. Constraining activity and growth substrate
568 of fungal decomposers via assimilation patterns of inorganic carbon and water into lipid biomarkers. Applied and
569 Environmental Microbiology, 90(4), e02065-23, 2024.

570 Kellermann, M. Y., Wegener, G., Elvert, M., Yoshinaga, M. Y., Lin, Y.-S., Holler, T., . . . Hinrichs, K.-U. Autotrophy as a
571 predominant mode of carbon fixation in anaerobic methane-oxidizing microbial communities. Proceedings of the National
572 Academy of Sciences, 109(47), 19321-19326. doi:10.1073/pnas.1208795109, 2012.

573 Kellermann, M. Y., Yoshinaga, M. Y., Wegener, G., Krukenberg, V., & Hinrichs, K.-U. Tracing the production and fate of
574 individual archaeal intact polar lipids using stable isotope probing. Organic Geochemistry, 95, 13-20.
575 doi:10.1016/j.orggeochem.2016.02.004, 2016. Kirk, T. K., & Farrell, R. L. Enzymatic" combustion": the microbial degradation
576 of lignin. Annual Reviews in
577 Microbiology, 41(1), 465-501. doi:10.1146/annurev.mi.41.100187.002341, 1987.

578 Kopf, S. H., Sessions, A. L., Cowley, E. S., Reyes, C., Van Sambeek, L., Hu, Y., ... & Newman, D. K. (2016). Trace
579 incorporation of heavy water reveals slow and heterogeneous pathogen growth rates in cystic fibrosis sputum. Proceedings of
580 the National Academy of Sciences, 113(2), E110-E116.

581 Kopf, S. H., McGlynn, S. E., Green-Saxena, A., Guan, Y., Newman, D. K., & Orphan, V. J. Heavy water and (15) N labelling
582 with NanoSIMS analysis reveals growth rate-dependent metabolic heterogeneity in chemostats. Environ Microbiol, 17(7),
583 2542-2556. doi:10.1111/1462-2920.12752, 2015.

584 Kornberg HL. Anaplerotic sequences in microbial metabolism. Angew Chem Int Ed Engl 4:558–565.
585 https://doi.org/10.1002/anie. 196505581, 1965.

586 Kreuzer-Martin, H. W. Stable isotope probing: linking functional activity to specific members of microbial communities. Soil
587 Science Society of America Journal, 71(2), 611-619, 2007..

588 Lekha, P. K., & Lonsane, B. K. Production and application of tannin acyl hydrolase: state of the art. Advances in applied
589 microbiology, 44, 215-260, 1997.

590 Lindahl, B. D., & Tunlid, A. Ectomycorrhizal fungi–potential organic matter decomposers, yet not saprotrophs. New
591 Phytologist, 205(4), 1443-1447. doi:10.1111/nph.13201, 2015.

592 Maloney, A. E., Kopf, S. H., Zhang, Z., McFarlin, J., Nelson, D. B., Masterson, A. L., & Zhang, X. Large enrichments in fatty
593 acid 2H/1H ratios distinguish respiration from aerobic fermentation in yeast Saccharomyces cerevisiae. *Proceedings of the*
594 *National Academy of Sciences*, *121*(20), e2310771121, 2024.

595 Osburn, M. R., Sessions, A. L., Pepe-Ranney, C., & Spear, J. R. Hydrogen-isotopic variability in fatty acids from Yellowstone
596 National Park hot spring microbial communities. Geochimica et Cosmochimica Acta, 75(17), 4830-4845, 2011.

597 Pilecky, M., Meador, T. B., Wassenaar, L.I. Advancements in Compound-Specific Hydrogen Stable-Isotope Analysis of Fatty
598 and Amino Acids. TrAC Trends in Analytical Chemistry, 118194. doi: 10.1016/j.trac.2025.118194, 2025.

599 Romanenko VI. Heterotrophic assimilation of CO2 by bacterial flora of water. Mikrobiologiia 33:679–683, 1964.

600 Roslev P, Larsen MB, Jørgensen D, Hesselsoe M. Use of heterotrophic CO2 assimilation as a measure of metabolic activity in
601 planktonic and sessile bacteria. J Microbiol Methods 59:381–393. https://doi.org/10. 1016/j.mimet.2004.08.002, 2004.

602 Sachse, D., Billault, I., Bowen, G. J., Chikaraishi, Y., Dawson, T. E., Feakins, S. J., ... & Kahmen, A. Molecular paleohydrology:
603 interpreting the hydrogen-isotopic composition of lipid biomarkers from photosynthesizing organisms. Annual Review of Earth
604 and Planetary Sciences, 40, 221-249, 2012.

605 Schinner F, Concin R, Binder H. Heterotrophic CO2 fixation by fungi in dependence on the concentration of the carbon source.
606 Paper presented at the Phyton; annales rei botanicae, 1982.

607 Schinner F, Concin R. Carbon dioxide fixation by wood-rotting fungi. Eur J For Pathol 11:120–123.

608 https://doi.org/10.1111/j.1439-0329. 1981.tb00077.x, 1981.

609 Sessions, A.L., Hayes, J.M., 2005. Calculation of hydrogen isotopic fractionations in biogeochemical systems. Geochim.

610 Cosmochim. Acta 69, 593–597.

611 Smith, S. E., & Read, D. Mineral nutrition, toxic element accumulation and water relations of arbuscular mycorrhizal plants.

612 Mycorrhizal symbiosis, 3, 145-148. doi:10.1016/B978-012370526-6.50007-6, 2008.

613 Šnajdr, J., Cajthaml, T., Valášková, V., Merhautová, V., Petránková, M., Spetz, P., . . . Baldrian, P. Transformation of Quercus

614 petraea litter: successive changes in litter chemistry are reflected in differential enzyme activity and changes in the microbial

615 community composition. FEMS Microbiology Ecology, 75(2), 291-303. doi:10.1111/j.1574-6941.2010.00999.x, 2011.

616 Sorokin, J. I. On the carbon dioxide uptake during the cell synthesis by microorganisms. Zeitschrift für allgemeine

617 Mikrobiologie, 6(1), 69-73. doi:10.1002/jobm.3630060107, 1966.

618 Sorokin, Y. I. Heterotrophic carbon dioxide assimilation by microorganisms. Zhurnal Obshchei Biologii, 22(4), 265272, 1961.

619 Treonis, A. M., Ostle, N. J., Stott, A. W., Primrose, R., Grayston, S. J., & Ineson, P. Identification of groups of metabolically-

620 active rhizosphere microorganisms by stable isotope probing of PLFAs. Soil Biology and Biochemistry, 36(3), 533-537, 2004.

621 Valentine, D. L. Isotopic remembrance of metabolism past. Proceedings of the National Academy of Sciences, 106(31), 12565-

622 12566. doi:10.1073/pnas.0906428106, 2009.

623 Warren, C. R. D2O labelling reveals synthesis of small, water-soluble metabolites in soil. *Soil Biology and Biochemistry*, *165*,

624 108543, 2022.

625 Wegener, G., Bausch, M., Holler, T., Thang, N. M., Prieto Mollar, X., Kellermann, M. Y., . . . Boetius, A. Assessing sub-seafloor

626 microbial activity by combined stable isotope probing with deuterated water and 13C-bicarbonate. Environmental

627 Microbiology, 14(6), 1517-1527. doi:10.1111/j.1462-2920.2012.02739.x, 2012.

628 Wegener, G., Kellermann, M. Y., & Elvert, M. Tracking activity and function of microorganisms by stable isotope probing of

629 membrane lipids. Current Opinion in Biotechnology, 41, 43-52. doi:10.1016/j.copbio.2016.04.022, 2016.

630 Wijker, R. S., Sessions, A. L., Fuhrer, T., & Phan, M. 2H/1H variation in microbial lipids is controlled by NADPH metabolism.

631 Proceedings of the National Academy of Sciences, 116(25), 12173-12182. doi:10.1073/pnas.1818372116, 2019.

632 Willers, C., Jansen van Rensburg, P. J., & Claassens, S. Phospholipid fatty acid profiling of microbial communities–a review

633 of interpretations and recent applications. Journal of applied microbiology, 119(5), 1207-1218, 2015.

634 Wu W, Meador T, Hinrichs K-U. Production and turnover of microbial organic matter in surface intertidal sediments.

635 Org Geochem 121:104–113. https://doi.org/10.1016/j.orggeochem.2018.04.006, 2018.

636 Wu, W., Meador, T. B., Könneke, M., Elvert, M., Wegener, G., & Hinrichs, K. U. Substrate-dependent incorporation of carbon

637 and hydrogen for lipid biosynthesis by Methanosarcina barkeri. Environmental Microbiology Reports, 12(5), 555567.

638 doi:10.1111/1758-2229.12876, 2020.

639 Zhang, X., Gillespie, A. L., & Sessions, A. L. Large D/H variations in bacterial lipids reflect central metabolic pathways.

640 Proceedings of the National Academy of Sciences, 106(31), 12580-12586. doi:10.1073/pnas.0903030106, 2009.